Polymer 235 (2021) 124277

Contents lists available at ScienceDirect

Polymer

journal homepage: www.elsevier.com/locate/polymer

Physicochemical characterization of the DNA complexes with different surfactants

Aleksandra Radko [a], Sebastian Lalik [a], Aleksandra Deptuch [b], Teresa Jaworska-Gołąb [a], Robert Ekiert [c], Natalia Górska [d], Katarzyna Makyła-Juzak [d], Jacek Nizioł [e], Monika Marzec [a,*]

[a] M. Smoluchowski Institute of Physics, Jagiellonian University, prof. S. Lojasiewicza 11, 30-348 Krakow, Poland
[b] Institute of Nuclear Physics Polish Academy of Sciences, Poland
[c] Faculty of Biochemistry, Biophysics and Biotechnology, Jagiellonian University, Poland
[d] Faculty of Chemistry, Jagiellonian University, Poland
[e] AGH University of Science and Technology, Faculty of Physics and Applied Computer Science, Poland

ARTICLE INFO

Keywords:
DNA complexes
X-ray diffraction
Dielectric spectroscopy

ABSTRACT

DNA complexes with cetyltrimethylammonium chloride (CTMA), benzyldimethylhexadecylammonium chloride (BAC) and hexadecylpyridinium chloride (HDP) surfactants as powder samples were studied by Fourier-transform middle infrared spectroscopy, X-ray diffraction and dielectric spectroscopy methods. Complexation as electrostatic interactions was confirmed by FT-MIR spectroscopy. The width of DNA-surfactant complexes was estimated to 61–73 Å based on modeling with the semi-empirical PM7 method. Based on SAXS results we propose the packing model for the complex molecules as hexagonal or slightly distorted hexagonal depending on the surfactant. For the first time the dielectric process registered in the low frequency range for all complexes was interpreted as oscillation of surfactant ions (BAC^+, HDP^+ or $CTMA^+$), analogous to the oscillation of ions (e.g. Na^+) in solutions of pure DNA. The influence of the structure of the complex-forming surfactant molecule on the value of the relaxation time distribution parameter is discussed.

1. Introduction

Deoxyribonucleic acid (DNA) is one of the most important biopolymers, because it carries genetic information in all living organisms. It forms a double-stranded, helical structure, with nitrogenous bases inside the helix and sugar-phosphate backbone on the outside. Such structure may adopt different conformations depending not only on the sequence of the bases, but also on the hydration and ionic environment. The most common B-conformation is a right-handed spiral characterized by 20 Å width. However, upon dehydration the structure becomes more compact but wider - the A-conformation of DNA is 23 Å wide [1]. Both structures contain two grooves along the helix, where proteins and small molecules can bind. Due to its importance, properties of DNA, in particular in aqueous environment, has already been well documented [2].

However, for the last two decades DNA is progressively attracting attention from researchers active in diverse areas closer to engineering and material sciences than to natural sciences or medicine. DNA or DNA-derived materials have been incorporated in a range of working electronic devices of improved characteristics. As an example can be quoted organic light emitting devices (OLED), organic field emission transistors (OFET), organic solar cells, devices for energy storage and numerous applications related to nonlinear optics (reviewed recently in Refs. [3–6]. Such kind of applications requires DNA prepared in form of solid, sub-micrometer layers. Because of its double helix structure, it is not a thermoplastic polymer. Therefore, the simplest and cost-effective techniques of DNA transformation involve solution processing. Unfortunately, the natural DNA is a highly hydrophilic biopolymer and therefore soluble only in water and water-based solvents. One of the ways to overcome this problem is to convert natural DNA into a complex soluble in common organic solvents.

The DNA possesses three unique features for creating functional complexes by interaction with small molecules. Being a polyelectrolyte, DNA is susceptible to electrostatic connections, has selective affinity for small molecules by intercalation, and binds specific molecules into its grooves. Therefore, DNA is an ideal template to fabricate highly ordered nanostructures by binding cationic agents such as cationic surfactants. Surfactants are molecules that consist of hydrophobic tail attached via a

* Corresponding Author.
E-mail address: monika.marzec@uj.edu.pl (M. Marzec).

https://doi.org/10.1016/j.polymer.2021.124277
Received 14 July 2021; Received in revised form 6 October 2021; Accepted 13 October 2021
Available online 15 October 2021

linker group to a hydrophilic head group which can carry electric charge. The association between DNA and cationic surfactant is of a great interest in basic research as well as in new fields of applications, for instance, the development of methods for DNA extraction and purification and potential use in drug- and gene-delivery systems. Various aspects of DNA association with cationic surfactants including complex formation, physicochemical characteristic of the structure, phase behavior and also a thermodynamic analysis of the interaction have been widely investigated using different methods (reviewed in Ref. [7]). The main driving force for the strong association between DNA and cationic surfactant is due to the electrostatic interactions between surfactant molecule and phosphate groups on the DNA strand. Additionally, the association between DNA and surfactant occurs as a result of the hydrophobic interactions between the alkyl chains of the surfactant molecules [7,8]. Due to the fact that surfactant structure is closely related to its interaction with DNA, studies of DNA association with different surfactants are interesting and necessary.

At present, there is still an ongoing debate concerning mechanisms responsible for the complexation process and its effect on the DNA structure. However, a consensus has been reached on the importance of the length of the aliphatic chain of the surfactant and the type of its charged head [9]. It has been demonstrated both experimentally and theoretically, that the most effective length of the aliphatic chain consists of sixteen carbons. Therefore, in this work, we decided to pursue this direction of research. We selected three cationic surfactants of this type and focused our attention on studying the effect of different nature of the charged head. The chosen surfactants were cetyltrimethylammonium chloride (CTMA), benzyldimethylhexadecylammonium chloride (BAC) and hexadecylpyridinium chloride (HDP). CTMA and BAC are both quaternary ammonium salts based on hexadecylamine. Amine group is additionally substituted with three methyl groups in CTMA, while BAC molecule possesses additional benzyl moiety and two methyl groups. In contrast, HDP structure is based on pyridinium salt which is additionally substituted with hexadecyl chain in the pyridine nitrogen atom. DNA-CTMA complex was considered as a reference material. In a sense, it is a standard material, most frequently used in organic electronics employing DNA derivatives. It can be efficiently deposited in form of thin films by various methods like spin casting [10,11], simple solvent evaporation [12] or the Langmuir-Blodgett method [13–18]. In addition, this compound has other interesting properties, for instance the ability to form spontaneously linear patterns if processed in a specific manner [15]. Nevertheless, dispersion of structural parameters observed within the same batch of DNA-CTMA complex is significant. This feature is explained by a range of competing phenomena occurring during the formation of micelles consisting of DNA helices surrounded by surfactant molecules.

Therefore, the goal of our study was to obtain an analogous material, but better organized in the bulk scale. The other two surfactants were chosen in the hope that the presence of the aromatic ring in the charged head would help to further stabilise the surfactant molecule. Such an effect could be achieved by binding the aromatic head in the DNA groove or, in the case of BAC, intercalation between planes defined in the helix by base pairs.

DNA-surfactant complexes in the form of powders (based on these three surfactants) were prepared and their properties were studied by means of Fourier transform middle-infrared spectroscopy (FT-MIR), X-ray diffraction and dielectric spectroscopy. The results obtained by FT-MIR allowed to assess the effectiveness of the complex formation, while the other two techniques allowed to conclude on the structural organization of the studied complexes at the microscopic level. The influence of the type of surfactant on the physical properties of the complex is discussed.

2. Materials

Low molecular weight DNA, cationic surfactants (benzyldimethylhexadecylammonium chloride, BAC ($CH_3(CH_2)_{15}N(Cl)(CH_3)_2CH_2C_6H_5$)), hexadecylpyridinium chloride, HDP ($C_{21}H_{38}ClN \cdot H_2O$); Tris base (tris(hydroxymethyl) aminomethane, cetyltrimethylammonium chloride, CTMA, ($CH_3(CH_2)_{15}N(Cl)(CH_3)_3$)) and hydrochloric acid (HCl) were used as received from SIGMA Aldrich. Molecular structure of surfactants used are presented in Fig. 1. DNA-surfactant complexes were synthesized in the following procedure:

1. Both DNA and the surfactants were dissolved in water in equal amounts (by weight), except for the BAC that was dissolved in twice as high concentration (at this concentration the yield of DNA-BAC complex formation was greatly improved).
2. The surfactant solution was added to the DNA solution drop-by-drop on a magnetic stirrer.
3. The received precipitate was thoroughly rinsed of excess surfactant with water and lyophilized in Christ Alpha 1–2 LDplus freeze dryer.
4. The complexes were obtained in the form of powders.

3. Methods

3.1. Fourier transform middle-infrared spectroscopy (FT-MIR)

Fourier transform middle-infrared absorption measurements (FT-MIR) were performed in transmission mode using a Bruker VERTEX 70v vacuum spectrometer. The spectra were carried out in the spectral range of 400–4000 cm^{-1} with a resolution of 2 cm^{-1} and 32 scans per each spectrum. Bulk samples of pure components: dried DNA, BAC, HDP, and CTMA surfactants as well as DNA–surfactant physical mixtures and DNA–surfactant complexes were mixed with KBr, compressed into pellets, and measured at room temperature.

3.2. X-ray diffraction (XRD)

Wide angle X-ray diffraction measurements for polycrystalline DNA-surfactant complexes (in borosilicate glass capillaries of 0.5 mm outer diameter) were carried out in the $2\theta = 2–40^\circ$ range with Empyrean 2 (PANalytical) diffractometer (CuKα radiation, parabolic mirror in the incident beam). A diffraction pattern of an empty capillary was used for background subtraction. Diffraction patterns of pure surfactants (flat samples) were collected in the $2\theta = 2–40^\circ$ range in the Bragg-Brentano geometry with the above mentioned diffractometer. Small-angle X-ray scattering (SAXS) measurements were performed in the $2\theta = 0.4–6.8^\circ$ range with Nanostar (Bruker) diffractometer (CuKα radiation). The results were analyzed using WinPLOTR [19] and Origin.

Molecular models of BAC, HDP, and CTMA ions were prepared in Avogadro [20] and optimized with the semi-empirical PM7 method in the Mopac2016 program [21,22].

3.3. Frequency domain dielectric spectroscopy (FDDS)

Dielectric spectra were collected by using the Turnkey Impedance Spectrometer Concept 81 (Novocontrol Technologies GmbH & Co. KG, Montabaur, Germany) at room temperature ($25.0 \pm 0.5\ ^\circ C$) in a broad frequency range of 0.5 Hz–3.0 MHz, at measuring voltage $V_m = 0.1V$. All pellet samples were placed in a flat rounded electrode capacitor (diameter of 9.60 mm). The thickness of each sample was determined by a micrometer screw (see Table 1) and was approximately the same for all samples (ca. 0.21–0.27 mm), except the DNA-HDP complex (ca. 0.89 mm). Due to the relatively hard and large fragments of the DNA-HDP sample, it was not possible to obtain a thinner pellet.

4. Results and discussion

4.1. FT-MIR studies

Infrared absorption spectroscopy has been applied in order to

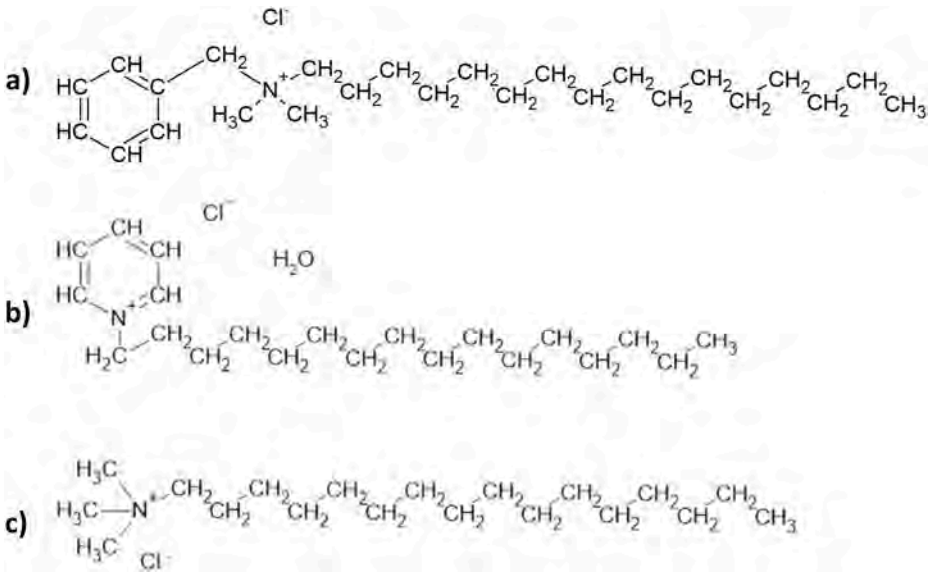

Fig. 1. Molecular structure of surfactants used: BAC (a), HDP (b), CTMA (c).

Table 1
The thickness of the studied DNA-surfactant and pure surfactant pellet samples.

Sample	Thickness [mm]
DNA-BAC	0.24(1)
DNA-HDP	0.89(1)
DNA-CTMA	0.22(1)
BAC	0.27(1)
HDP	0.21(1)
CTMA	0.25(1)

confirm proper chemical composition of all components used in preparation of the DNA–BAC and DNA–HDP complexes and to validate their formation. The results obtained in this study for the two complexes are also compared with the results published previously by us for the DNA–CTMA complex [15]. Comparisons of IR spectra of pure DNA, BAC, HDP and CTMA compounds as well as two-component DNA–surfactant mixtures and complexes are presented in Fig. 2. The spectrum of pure DNA confirms its B-conformation as the characteristic bands, which are spectroscopic markers for this form of DNA, are observed at 831, 966 and 1224 cm^{-1} [23,24]. The most significant changes in positions of IR bands in the spectra of DNA-surfactant complexes in comparison to pure components and two-component mixtures (obtained by simple mixing equal amounts by weight of DNA and surfactant) are summarized in Table 2. The appearance of new bands in the spectra are also included. Shifts of some bands and their different shapes observed in the spectra of all complexes comparing to the single components and mixtures are very consistent.

The band, which is the most sensitive to environmental and structural changes upon complexation, is the one connected to the $\nu_{as}(PO_2^-)$ vibration. In our study the shift of this band towards larger wavenumbers (above 1240 cm^{-1}) is observed for all DNA-surfactant complexes confirming their creation and suggesting that A-DNA conformation is predominant. The band shape in the spectral range of 1080–1120 cm^{-1}, where the $\nu_s(PO_2^-)$ vibration is present, is also modified. In the case of the DNA–BAC and DNA–HDP complexes, more prominent and separate band is visible at 1092 and 1095 cm^{-1}, respectively, which is also indicative of complex formation. In spectrum of pure DNA as well as DNA–surfactant mixtures only broadening in this region is observed.

Summing up, the changes observed in the IR spectra of the DNA–BAC and DNA–HDP complexes by comparing them with the spectra of pure

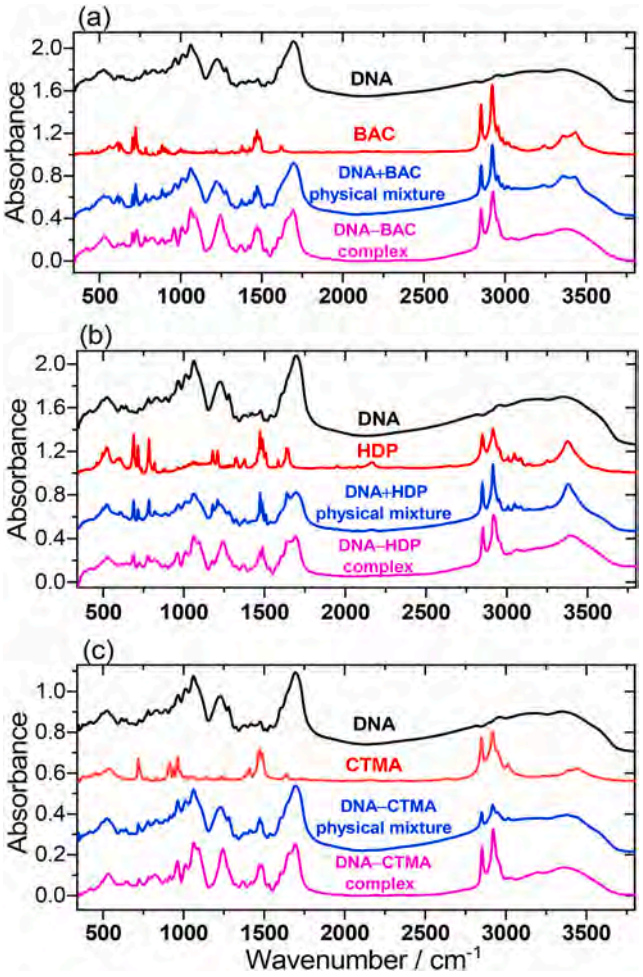

Fig. 2. FT-MIR spectra of pure components (DNA, BAC, HDP and CTMA), DNA–surfactant physical mixtures and complexes: DNA–BAC (a), DNA–HDP (b) and DNA–CTMA (c).

Table 2
Changes in bands' positions (in cm^{-1}) in the IR spectra of DNA–surfactant complexes in comparison to pure components with their tentative assignment based on literature [18,23,25,26].

DNA	BAC	HDP	CTMA	DNA–BAC	DNA–HDP	DNA–CTMA	Tentative assignment
524				529	529	533	ring deformation in adenine
642				647	647	648	
	723 shp		719	728 br		722	$\rho(CH_2)_{al,n}$
831[B]				823		824	phosphodiester
966[B]				959	959	962	δ(O–P–O)/C–C and C–O of DNA backbone
1013				1008	1009	1010	ν(C–O) in sugar ring
~1090 sh				1092 shp	1095 shp	1093 shp	$\nu_s(PO_2^-)$
1224[B]				1244[A]	1243[A]	1243[A]	$\nu_{as}(PO_2^-)$
1280[B]				1277	1278	1277	deoxyribose-thymine
			1471			1468	$\delta(CH_2)_{al}$
	1471	1472		1468	1468		ν(C═C)$_{ar}$
	1490			1485			ν(C═C)$_{ar}$
1538				1528	1529	1529	deoxycytidine
–				1573	1573	1574	
		2849	2849		2851	2852	$\nu_s(CH_2)_{al}$
	2921	2914	2917	2924	2920	2921	$\nu_{as}(CH_2)_{al}$

[A or B] Positions of IR bands characteristic for different conformations of DNA (A or B).
Modes' description: ν – stretching; δ – bending; r – rocking; s – symmetric; as – asymmetric; ar – aromatic; al – aliphatic; n – long chain; sh – shoulder; shp – sharp; br – broad.

components and mixtures indicate effective interactions between DNA and cationic surfactant (BAC or HDP). The molecular structure of DNA used in this study has been moderately modified by both BAC and HDP surfactants indicating creation of complexes based on electrostatic interactions between the surfactant's polar head group and the phosphate backbones of DNA. Analogical modifications in the IR spectrum, due to the formation of the complex (lipoplex), have been previously seen by us for DNA–CTMA complex [15,16].

The FT-MIR results also showed that for the native form of DNA (derived from salmon sperm), the B-DNA conformation is dominant, while for the complexes, the A-DNA conformation. We believe that this conformational change is induced by interactions between the surfactant and DNA molecules (leading to the formation of a DNA-surfactant complex), although the exact mechanism of this phenomenon has not been elucidated so far.

4.2. XRD studies

Wide angle X-ray diffraction patterns collected at room temperature (Fig. 3a) consist of a low-angle peak or peaks in the $2\theta = 2–6^\circ$ range and a hump about 20°. The former are visible for complexes but not for the pure low molecular weight DNA. The latter, appearing also in the XRD patterns of native DNA (see the bottom pattern in Fig. 3a and ref. [27]), corresponds to the average distance of 4.4–4.5 Å. Due to the large half-width of the maximum, it can be attributed to the distribution of intra-molecular distances within DNA helix and, for complexes, also to distances between long carbon chains of surfactant molecules. It should be noticed that for the complexes very low intensity sharp peaks are visible on the hump (Fig. 3a), indicating the presence of some small amount of surfactants (not complex forming) in the samples (XRD patterns of the surfactants consist of numerous sharp peaks, see Fig. S1).

For precise analysis of the low-angle region, SAXS measurements were performed both for the complexes and the surfactants (Fig. 3b) and these results were used for further analysis. The patterns of DNA-BAC, DNA-HDP and DNA-CTMA contain small peaks at $2\theta = 4.2^\circ$, 3.1° and 3.4°, respectively, which originate from small amount of free surfactants present in the samples mentioned above. The structure of complexes should be therefore derived only from the strong peaks at $2\theta = 2–2.5^\circ$, which are observed neither in the pattern of pure DNA nor in the patterns of pure surfactants. For DNA-BAC and DNA-HDP, the SAXS patterns reveal three overlapping peaks in the $2\theta = 2–2.5^\circ$ range and for DNA-CTMA only a single maximum is there observed.

The characteristic distances in complexes determined from the positions of the low-angle peaks in the SAXS patterns (using the Bragg

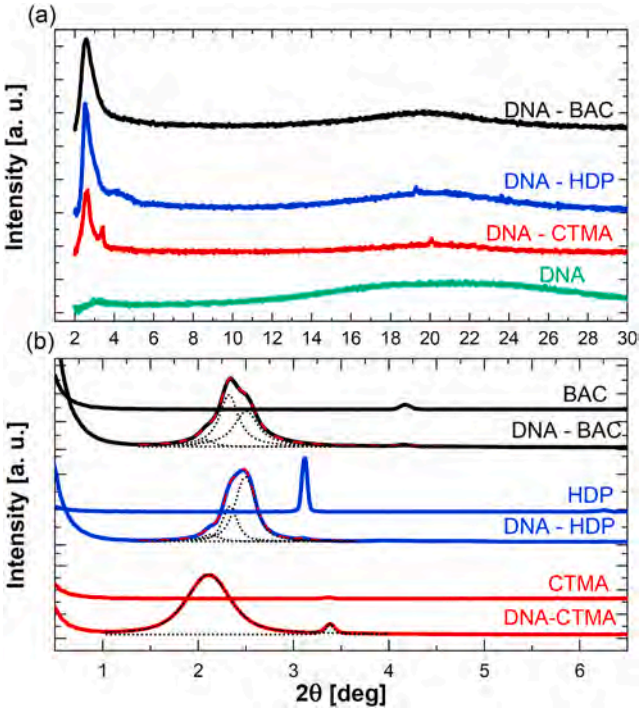

Fig. 3. Wide angle XRD patterns of pure DNA and its complexes with BAC, HDP, and CTMA (a) and SAXS patterns of the investigated DNA complexes compared with respective pure surfactant (b).

Table 3
Ion length L of surfactants, estimated molecular width W_A+2L and the characteristic distances D (determined experimentally by SAXS) of each DNA complex.

		estimated molecular width		characteristic distance
surfactant	L [Å]	$W_A + 2L$ [Å]*	$(W_A + 2L)/2$ [Å]	D [Å]
BAC	25.2	73.4	36.7	42.4(5); 38.0(1); 35.2(3)
HDP	22.7	68.4	34.2	41(2); 37.8(3); 35.4(3)
CTMA	21.3	65.6	32.8	41.9(1)

*W_A = 23 Å is the helix width of the A-DNA.

equation) are collected in Table 3. To compare these distances with appropriate widths of DNA complexes, the ions of BAC, HDP and CTMA surfactants were modeled with the semi-empirical PM7 method and the results are presented in Fig. 4. The length of ions was determined as the distance between the most distant non-hydrogen atoms, the width of DNA helix was taken as $W_{DNA} = 23$ Å, the value for the A-form of DNA [1], as this form was confirmed by the FT-MIR measurements presented above. It was assumed that surfactant molecules attach to the DNA helix on both sides [25,27]. The width of the DNA complex is calculated considering that surfactant molecules are in the most extended conformation. Therefore, generally it can be smaller, as the long carbon chains are flexible and can take also numerous bend conformations. The estimated width of the studied DNA complexes is about 70 Å (Table 3) and divided by two gives the value close to the distances determined from the strongest peaks in the $2\theta = 2$–2.5° range for DNA-BAC and DNA-HDP. For DNA-CTMA, the single low-angle peak corresponds to a larger distance of 42 Å, which implies not so dense structure of this complex.

Considering the data collected in Table 3, we propose for the studied complexes of low molecular weight DNA a simple model of packing described by a two-dimensional rectangular centered lattice, visualized in Fig. 5. In the DNA-CTMA complex there is only one strong diffraction peak in the low-angle region, which implies that the packing is hexagonal (resembling inverse hexagonal packing presented in Fig. 1b in Ref. [28]) and the lattice parameters satisfy the relationship $b = a\sqrt{3}$. In this case, the peak at $2\theta = 2.1^\circ$ can be indexed both by (02) and (11) Miller indices and the obtained lattice parameters are $a = 48.3(1)$ Å and $b = 83.7(2)$ Å. The a lattice constant is also the distance between the nearest-neighbor DNA helices.

The structure of DNA-BAC and DNA-HDP complexes can be described as a slightly distorted hexagonal structure, resembling the one shown in Fig. 5, but with the $b = a\sqrt{3}$ condition not exactly fulfilled. In consequence the positions of the (02) and (11) peaks do not coincide. Additionally, the (11) peak is stronger than (02), as it contains contribution both from the (11) and $(1\bar{1})$ planes. Taking these into account, the unit cell parameters can be calculated as $a = 45.1(3)$ Å and $b = 70.5(5)$ Å ($b = 1.56a$) for DNA-BAC and $a = 40.0(6)$ Å and $b = 75.7(6)$ Å ($b = 1.89a$) for DNA-HDP. The smallest maximum in the deconvolution of the peak at $2\theta = 2.1^\circ$ in the SAXS patterns of DNA-BAC and DNA-HDP has similar position as the strong peak in the pattern of DNA-CTMA. That allows to understand it as originating from a small volume of hexagonal phase developed in these complexes ($a = 48.9(6)$ Å, $b = 85(1)$ Å for DNA-BAC and $a = 48(2)$ Å, $b = 83(4)$ Å for DNA-HDP).

4.3. FDDS studies

Permittivity (ε^*) is a complex quantity and its real (ε') and imaginary (ε'') parts could be determined by using the impedance spectroscopy where capacity (C) and loss tangent ($tg\delta = \varepsilon''/\varepsilon'$) are measured. Also, the real and imaginary parts of the complex impedance (Z^*) and complex conductivity (σ^*) could be calculated. These quantities are related to each other according to the formulas gathered in Table 4.

Dielectric spectra have been measured for all of the DNA-surfactant samples as well as pure surfactants at room temperature. Fig. 6 presents dielectric absorption and dispersion together with the electric conductivity for all created complexes. Out of all three DNA complexes studied, DNA-BAC complex shows the lowest dielectric dispersion and absorption in the whole frequency range (Fig. 6a and b). The drastic increase of ε' and ε'' with decreasing measuring frequency can be associated with the electrode polarization phenomenon or some relaxation process at sub-hertz region. As it is visible in Fig. 6c the electric conductivity increases with increasing frequency for all the complexes. As an example ε' together with the conductivity σ' at 0.5 Hz for all the samples are gathered in Table 5. For DNA-BAC complex the conductivity value is about 5 times smaller than for both DNA-HDP and DNA-CTMA complexes and ε' is also the lowest for this complex.

According to Baker-Jarvis et al. [29], several relaxation processes in DNA sample can be registered by dielectric spectroscopy. The relaxation occurring in the megahertz region is related to the movement of condensed counter ions associated with individual phosphate groups. There are also other processes in the very high frequency range, but we do not discuss them here because they are outside the measuring range in our studies. On the other hand, the relaxation that occurs at low frequencies (usually in the range 1–100 Hz) is related to the longitudinal polarization of the diffusion counter ion shell that surrounds the molecule. In the case of all three complexes studied, only a drastic increase in dielectric absorption is visible (Fig. 6b). This seems to be attributable to the aforementioned low frequency relaxation process if the presence of a large surfactant molecule bound to the DNA helix would shift the frequency of this process to a lower frequency range, below 1 Hz. In order to check our hypothesis, the dielectric results are presented in the impedance representation (Fig. 7) in which the relaxation processes are shifted towards higher frequencies in relation to the permittivity representation [30]. As can be seen, the low frequency relaxation process is very clearly visible in this representation for all three complexes studied. The following Cole-Cole model was fitted to the experimental data ($Z'(f)$ and $Z''(f)$) [26,31,32]:

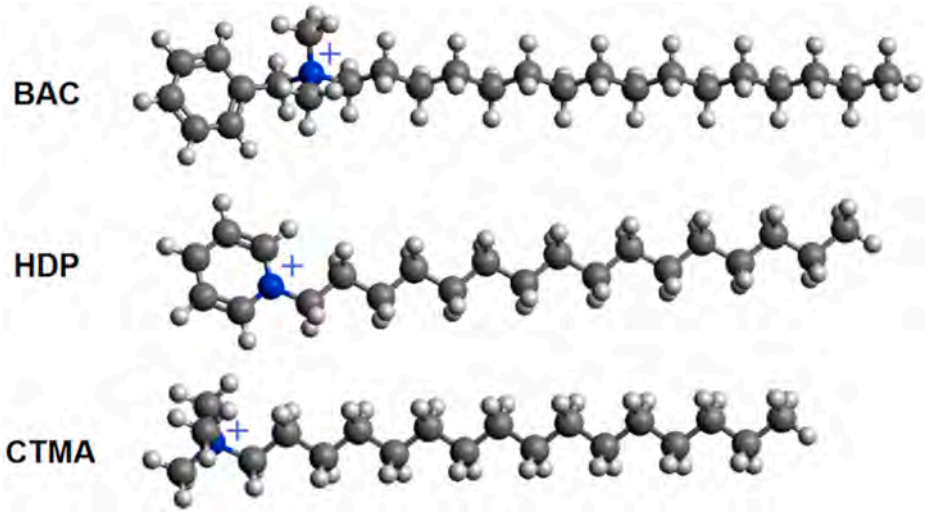

Fig. 4. BAC, HDP, and CTMA ions optimized with PM7 method in Mopac2016 and visualized in Avogadro.

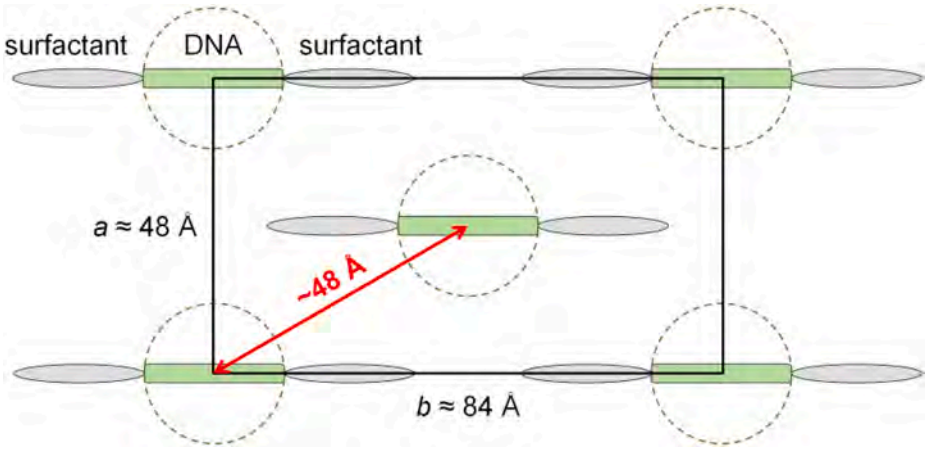

Fig. 5. Hexagonal packing model of DNA complexes. The picture shows the intersection perpendicular to the DNA helices that are perpendicular to the Figure. In a volume sample the surfactant molecules surround the DNA helix in a manner resembling a hairy caterpillar.

Table 4
Formulas describing the permittivity, impedance and conductivity.

	Formula
Permittivity	$\varepsilon^* = \varepsilon' - i\varepsilon''$
Impedance	$Z^* = Z' + iZ''$
	$Z'(f) = \frac{1}{2\pi f C_0} \frac{\varepsilon''(f)}{(\varepsilon'(f))^2 + (\varepsilon''(f))^2}$
	$Z''(f) = -\frac{1}{2\pi f C_0} \frac{\varepsilon'(f)}{(\varepsilon'(f))^2 + (\varepsilon''(f))^2}$
Conductivity	$\sigma^* = \sigma' + i\sigma''$
	$\sigma'(f) = 2\pi f \varepsilon_0 \varepsilon''(f) = \sigma_{DC} + \sigma_{AC}(f)$
	$\sigma''(f) = 2\pi f \varepsilon_0 \varepsilon'(f)$

i – imaginary unit, f – frequency, C_0 - capacity of empty capacitor used, ε_0 - vacuum dielectric permittivity, σ_{DC}, σ_{AC} – direct and alternative electric conductivity.

$$Z^*(f) = Z'_\infty + \frac{Z'_s - Z'_\infty}{1 + \left(\frac{2\pi i f}{f_R}\right)^{1-\alpha}} = Z'_\infty + \frac{\Delta Z'}{1 + \left(\frac{2\pi i f}{f_R}\right)^{1-\alpha}} \quad (1)$$

where Z'_s, Z'_∞ are impedance at low and high frequency limit, ΔZ'- impedance increment, f_R - relaxation frequency, α – the distribution parameter of relaxation time ($0 < \alpha < 1$).

As an example, the results of fitting Eq. (1) to the experimental data registered for DNA-BAC complex is presented in Fig. 7d as solid line while impedance increment $\Delta Z'$, relaxation frequency f_R and α parameter obtained by fitting procedure for all three complexes studied are gathered in Table 6. As can be seen these parameters are different for each complex what means that each of the surfactant has different influence on the relaxation process observed. The weakest process (the lowest $\Delta Z'$) registered for DNA-CTMA complex has the lowest relaxation frequency (ca. 4.87 Hz) and the highest α parameter (ca. 0.385). In the case of DNA-BAC and DNA-HDP complexes the α parameter is small and on the Euler-Argand plot (Fig. 7c) this relaxation process is presented as almost like a semicircle centered on the Z' axis (Debye type process). In turn, the higher α parameter for DNA-CTMA complex proves the non-Debye nature of this process and on the Euler-Argand plot shows a part of the circle with the center shifted below the Z' axis (see Table 6 and Fig. 7c). For DNA-HDP and DNA-BAC complexes α parameter is ca. 1.4 and 2 times lower than for DNA-CTMA, accordingly. It means that presence of an aromatic ring in BAC and HDP surfactants leads to decrease in the distribution parameter of relaxation time in the complexes formed by these surfactants. This effect may indirectly indicate an increased structural homogeneity of these complexes.

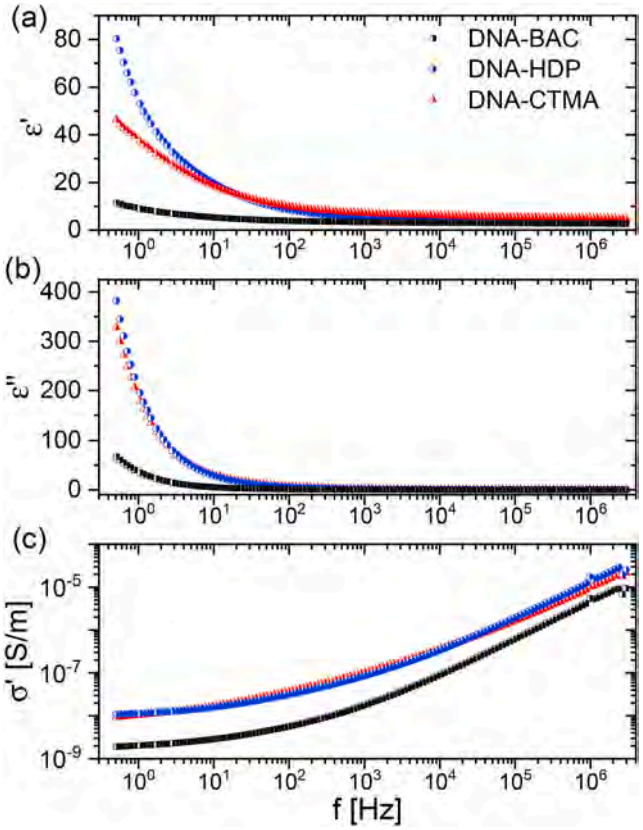

Fig. 6. Dielectric dispersion (a), absorption (b), and electric conductivity (c) of the studied DNA-surfactant complexes. The legend in (a) is the same for all graphs.

Table 5
Real part of permittivity and electric conductivity at f = 0.5 Hz for complexes studied.

	ε'	σ' [nS/m]
DNA – BAC	11.41	1.90
DNA – HDP	46.21	10.87
DNA – CTMA	80.38	9.33

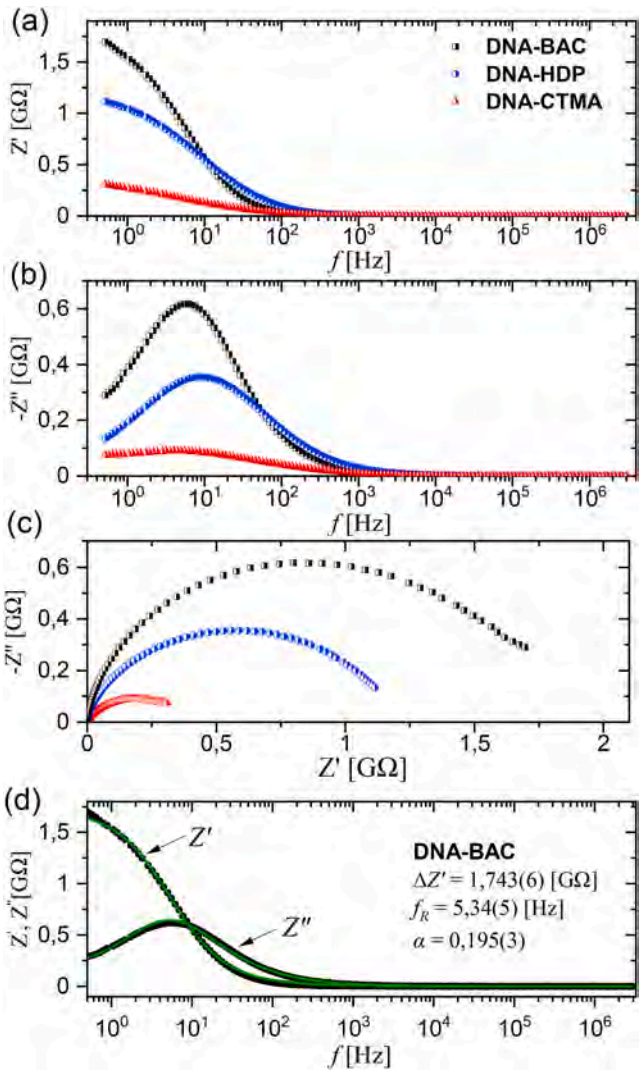

Fig. 7. The real (a) and imaginary (b) part of impedance, the Euler-Argand plot for DNA-surfactant complexes studied (c) and impedance spectrum for DNA-BAC with fitting results as solid line (d). The legend in (a) is the same for (a – c) graphs.

Table 6
Impedance increment $\Delta Z'$, α parameter and relaxation frequency f_R obtained from the fitting Eq. (1) to the experimental data.

	$\Delta Z'$ [GΩ]	f_R [Hz]	α
DNA – BAC	1.743(6)	5.34(5)	0.195(3)
DNA – HDP	1.173(4)	8.71(8)	0.286(2)
DNA – CTMA	0.349(2)	4.87(9)	0.385(3)

As is known, the interaction of the counter ions with the pure DNA molecule is complex. Some of the counter ions are bound to the phosphate backbone by a weak covalent chemical bond, while others are more loosely bound and can move around [29]. The counter ions are attracted to the backbone of negative phosphate charges and form a counter ion shell that screens some of the DNA's charge, as a result the double layer is formed. These counter ions are somewhat mobile and oscillate around the phosphate charge centers in the measuring electric field applied, so the relaxation in the low frequency range is visible [29]. Although we study DNA-surfactant complexes, we believe that the double layer for complexes forms similarly. Since there is a surfactant here, the formation of double layer can occur near the DNA helix as for pure DNA between negatively charged phosphate groups and functional group of the surfactant (Fig. 8). We suppose that the oscillations of the functional group (surfactant) in the measuring electric field may be responsible for the relaxation process registered for all complexes (Fig. 7).

To validate our concept, the dielectric spectra of pure surfactants were measured as well. In the case of CTMA and HDP surfactants the dispersion curves $\varepsilon'(f)$ are very similar but the HDP curve is shifted towards higher ε' values by about 0.3 in the whole frequency range (Fig. 9a). Moreover, there is not visible any relaxation process for pure surfactants in the permittivity (Fig. 9a and b) as well as in the impedance representation (Fig. 9c). For DNA-surfactant complexes studied the Z' values at 0.5 Hz are lower compared to pure surfactants (see Table 7).

As can be seen in Fig. 9d, BAC surfactant exhibits the highest electric conductivity in the frequency range up to 100 kHz while the conductivity of CTMA and HDP surfactants are equal in the range up to 10 kHz. The conductivity is higher for BAC in comparison to CTMA and HDP in a wide frequency range. Interestingly, conductivity of pure surfactants is lower than for DNA-surfactant complexes (see Table 7). In order to explain the differences in conductivity, we should refer to the chemical structure of surfactants (Fig. 4). All of them have the same aliphatic chain from right-hand side, namely $-(CH_2)_{15}CH_3$ while for BAC and HDP from the left-hand side an aromatic ring is attached. Additionally, all surfactants have a nitrogen atom in the structure, which is in different position. It seems that the conductivity strongly depends on the position of the nitrogen atom, but it requires further studies.

5. Conclusions

DNA complexes with various surfactants in the form of powder samples were studied by FT-MIR and dielectric spectroscopy as well as XRD methods. The FT-MIR measurements confirmed the effective formation of DNA complex in the case of all three surfactants (BAC, CTMA and HDP). The results suggest the majority of electrostatic interactions in the complex formation process. It was also found that after the complexation DNA changes its conformation from native B-conformation to A-conformation.

XRD measurements and modeling with the semi-empirical PM7 method allowed to estimate the width of the DNA complexes to 61–73 Å in case of fully extended alkyl chains. We propose the packing model for the complex molecules of the surfactants studied as hexagonal for DNA-CTMA and distorted-hexagonal for DNA-BAC and DNA-HDP.

Dielectric studies of the complexes showed the existence of one relaxation process with a relaxation frequency lower than that observed usually in DNA solutions. We suppose that the complexes are similar to

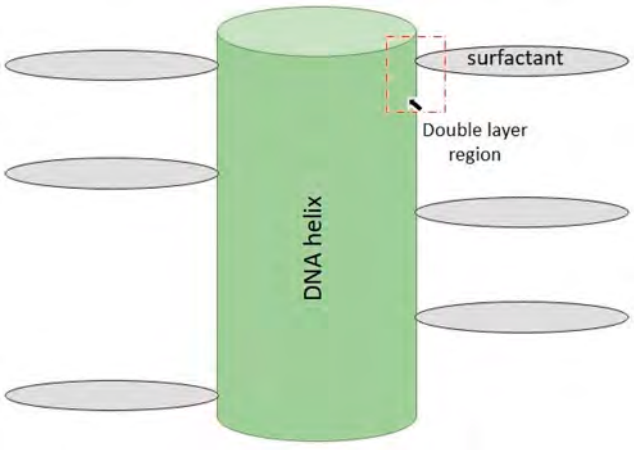

Fig. 8. Model of double layer region formation between DNA and surfactant molecules.

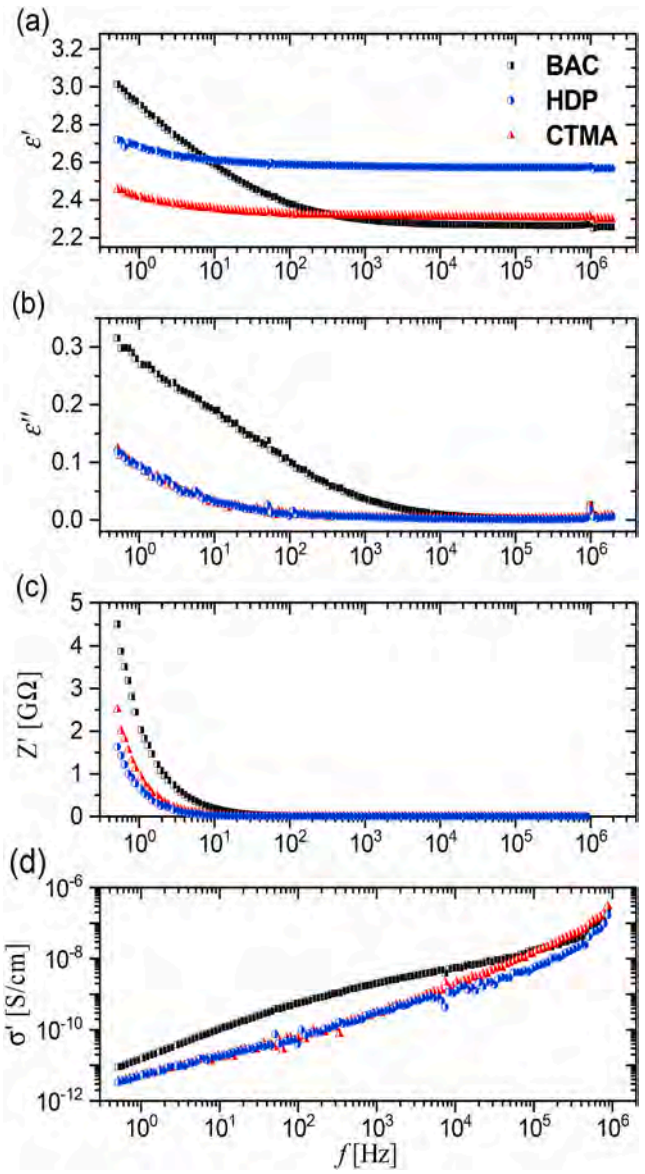

Fig. 9. The real (a) and imaginary (b) part of permittivity as well as the real parts of impedance (c) and electric conductivity (d) of surfactants. The legend in (a) is the same for all graphs.

Table 7
Real part of impedance Z' and electric conductivity σ' at 0.5 Hz of pure surfactants and complexes; σ_C - conductivity of complex, σ_S - conductivity of surfactant.

	DNA-BAC	BAC	DNA-HDP	HDP	DNA-CTMA	CTMA
Z' [GΩ]	4.51	1.70	1.63	1.11	2.51	0.31
σ' [pS/m]	1900	8.98	10870	3.37	9330	3.55
σ_C/σ_S	211.58		3225.52		2628.17	

pure DNA in solution in respect of formation of double layer, however, the counter ion is not a simple ion but a complex system (BAC^+, HDP^+ or $CTMA^+$). Thus, the low frequency process registered for all three complexes has the same origin as the process in DNA solutions, while the shift in the relaxation frequency towards lower values is related to the oscillation of a much larger object than the counter ion like Na^+. It seems to be confirmed by XRD results. Another important conclusion is that the presence of an aromatic ring in BAC and HDP surfactants leads to decrease in the distribution parameter of relaxation time in the DNA-BAC and DNA-HDP complexes, which may indirectly indicate an increase in the structural homogeneity of these complexes compared to the DNA-CTMA complex, where this ring is absent.

CRediT authorship contribution statement

Aleksandra Radko: Conceptualization, Writing – original draft, preparation, Visualization, Investigation, Data curation. **Sebastian Lalik:** Visualization, Investigation, Data curation. **Aleksandra Deptuch:** Visualization, Investigation, Data curation. **Teresa Jaworska-Gołąb:** Visualization, Investigation, Data curation. **Robert Ekiert:** Writing – original draft, preparation, Validation, Methodology, Writing – review & editing. **Natalia Górska:** Visualization, Investigation, Data curation. **Katarzyna Makyła-Juzak:** Writing – original draft, preparation, Writing – review & editing, Validation, Methodology. **Jacek Nizioł:** Writing – review & editing. **Monika Marzec:** Validation, Methodology, Writing – review & editing, Founding, Supervision.

Declaration of competing interest

The authors declare that they have no known competing financial interests or personal relationships that could have appeared to influence the work reported in this paper.

Acknowledgments

The authors are indebted to Professor Damian Pociecha (Faculty of Chemistry, University of Warsaw, Poland) for SAXS measurements. This publication has been funded from the SciMat Priority Research Area budget under the Strategic Programme Excellence Initiative at the Jagiellonian University) (contract no. PSP U1U/P05/NW/03.18).

Empyrean 2 (PANalytical) diffractometer was purchased thanks to European Regional Development Fund Operational Program Infrastructure and Environment (contract no. POIS.13.01.00-00-062/08).

The research was carried out with the equipment (Novocontrol Spectrometer) purchased thanks to the financial support of the European Regional Development Fund in the framework of the Polish Innovation Economy Operational Program (contract no. POIG.02.01.00-12-023/08).

Appendix A. Supplementary data

Supplementary data to this article can be found online at https://doi.org/10.1016/j.polymer.2021.124277.

References

[1] D.W. Ussery, DNA structure: A-, B- and Z-DNA helix families, in: Encyclopedia of Life Sciences, 2002, https://doi.org/10.1038/npg.els.0003122.
[2] R.R. Sinden, DNA structure and function, DNA Structure and Function (2012) 1–398, https://doi.org/10.1016/C2009-0-02451-9.
[3] F. Gomez Eliot, J. Steckl Andrew, Engineering DNA and nucleobases for present and future device applications, in: M. Irimia-Vladu, E.D. Glowacki, N.S. Sariciftci, S. Bauer (Eds.), Green Materials for Electronics, Wiley-VCH, 2018, pp. 199–233.
[4] Y. Kawabe, DNA-based dye lasers: progress in this half a decade, Nanobiosystems: Processing, Characterization, and Applications IX (2016), https://doi.org/10.1117/12.2237439, 9928, 992806.
[5] N. Kobayashi, K. Nakamura, DNA electronics and photonics. *Electronic Processes in organic electronics: bridging nanostructure*, Electronic States and Device Properties (2015) 253–281, https://doi.org/10.1007/978-4-431-55206-2_12.
[6] N. Ogata, DNA as material, in: K. Mizoguchi, H. Sakamoto (Eds.), DNA Engineering. Properties and Applications, Pan Stanford Publishing, 2017, pp. 257–276.
[7] K. Liu, L. Zheng, C. Ma, R. Göstl, A. Herrmann, DNA-surfactant complexes: self-assembly properties and applications, Chem. Soc. Rev. 46 (16) (2017) 5147–5172, https://doi.org/10.1039/c7cs00165g.
[8] C.H. Spink, J.B. Chaires, Thermodynamics of the binding of a cationic lipid to DNA, J. Am. Chem. Soc. 119 (45) (1997) 10920–10928, https://doi.org/10.1021/JA964324S.
[9] R. Dias, K. Dawson, M.G. Miguel, Interaction of DNA with surfactants in solution, in: R.S. Dias, B. Lindman (Eds.), DNA Interactions with Polymers and Surfactants, Wiley, 2008, pp. 89–117.

[10] J.A. Hagen, W. Li, A.J. Steckl, J.G. Grote, Enhanced emission efficiency in organic light-emitting diodes using deoxyribonucleic acid complex as an electron blocking layer, Appl. Phys. Lett. (2006), https://doi.org/10.1063/1.2197973.
[11] E. Hebda, M. Jancia, F. Kajzar, J. Niziol, J. Pielichowski, I. Rau, A. Tane, Optical properties of thin films of DNA-CTMA and DNA-CTMA doped with nile blue, Mol. Cryst. Liq. Cryst. 556 (1) (2012) 309–316, https://doi.org/10.1080/15421406.2012.642734.
[12] L. Wang, J. Yoshida, N. Ogata, S. Sasaki, T. Kajiyama, Self-assembled supramolecular films derived from marine deoxyribonucleic acid (DNA) - cationic surfactant complexes: large-scale preparation and optical and thermal properties. Chemistry of Materials, 2001, https://doi.org/10.1021/cm000869g.
[13] L.K. Brar, P. Rajdev, A.K. Raychaudhuri, D. Chatterji, Langmuir monolayer as a tool toward visualization of a specific DNA-protein complex, Langmuir 21 (23) (2005) 10671–10675, https://doi.org/10.1021/la051062b.
[14] J. Lee, C.H. Chang, The interaction between the outer layer of a mixed ion pair amphiphile/double-chained cationic surfactant vesicle and DNA: a Langmuir monolayer study, Soft Matter 10 (11) (2014) 1831–1839, https://doi.org/10.1039/c3sm52276h.
[15] J. Nizioł, K. Makyła-Juzak, A. Radko, R. Ekiert, J. Zemła, N. Górska, A. Chachaj-Brekiesz, M. Marzec, H. Harańczyk, P. Dynarowicz-Latka, Linear, self-assembled patterns appearing spontaneously as a result of DNA-CTMA lipoplex Langmuir-Blodgett deposition on a solid surface, Polymer 178 (2019), https://doi.org/10.1016/j.polymer.2019.121643.
[16] A. Radko, J. Nizioł, K. Makyła-Juzak, R. Ekiert, N. Górska, A. Górecki, M. Marzec, Properties of DNA-CTMA monolayers obtained by Langmuir-Blodgett technique. Materials Science and Engineering B: Solid-State Materials for Advanced Technology, 2021, https://doi.org/10.1016/j.mseb.2020.114859.
[17] S. Tassler, B. Dobner, L. Lampp, R. Ziółkowski, E. Malinowska, C. Wölk, G. Brezesinski, DNA delivery systems based on peptide-mimicking cationic lipids - the effect of the Co-lipid on the structure and DNA binding capacity, Langmuir 35 (13) (2019) 4613–4625, https://doi.org/10.1021/acs.langmuir.8b04139.
[18] Yunfei He, Y. He, Study on the interfacial properties of surfactants and their interactions with DNA, PhD Thesis, https://tel.archives-ouvertes.fr/tel-00852186/document, 2013.
[19] T. Roisnel, J. Rodríguez-Carvajal, WinPLOTR: a windows tool for powder diffraction pattern analysis. Materials Science Forum, 2001. https://doi.org/10.4028/www.scientific.net/msf.378-381.118.
[20] M.D. Hanwell, D.E. Curtis, D.C. Lonie, T. Vandermeerschd, E. Zurek, G. R. Hutchison, Avogadro: an advanced semantic chemical editor, visualization, and analysis platform, J. Cheminf. (2012), https://doi.org/10.1186/1758-2946-4-17.
[21] J.J.P. Stewart, Optimization of parameters for semiempirical methods VI: more modifications to the NDDO approximations and re-optimization of parameters, J. Mol. Model. (2013), https://doi.org/10.1007/s00894-012-1667-x.
[22] J.J.P. Stewart, MOPAC2016 (Stewart Computational Chemistry, Colorado Springs, CO, USA), 2016, Stewart Computational Chemistry, Colorado Springs, CO, USA, 2016.
[23] C.S. Braun, G.S. Jas, S. Choosakoonkriang, G.S. Koe, J.G. Smith, C.R. Middaugh, The structure of DNA within cationic lipid/DNA complexes, Biophys. J. (2003), https://doi.org/10.1016/S0006-3495(03)74927-3.
[24] M.L.S. Mello, B.C. Vidal, Changes in the infrared microspectroscopic characteristics of DNA caused by cationic elements, different base richness and single-stranded form, PLoS One 7 (8) (2012), https://doi.org/10.1371/JOURNAL.PONE.0043169.
[25] L. Liang, Y. Fu, D. Wang, Y. Wei, N. Kobayashi, T. Minari, DNA as functional material in organic-based electronics, Appl. Sci. 8 (1) (2018), https://doi.org/10.3390/app8010090.
[26] F. Kremer, A. Schönhals, Springer-Verlag Berlin Heidelberg GmbH. https://doi.org/10.1007/978-3-642-56120-7, 2002.
[27] J. Nizioł, R. Ekiert, M. Śniechowski, M. Słomiany, M.M. Marzec, Thermally forced transitions of DNA-CTMA complex microstructure, Opt. Mater. 56 (2016) 84–89, https://doi.org/10.1016/j.optmat.2016.01.049.
[28] R. Krishnaswamy, V.A. Raghunathan, A.K. Sood, Reentrant phase transitions of DNA-surfactant complexes, APS 69 (3 1) (2004), https://doi.org/10.1103/PhysRevE.69.031905.
[29] J. Baker-Jarvis, C.A. Jones, B. Riddle, Electrical properties and dielectric relaxation of DNA in solution, in: NIST Technical Note, 1998.
[30] Stanisław Urban, et al., Dielectric studies in the isotropic phase of six symmetrical azomethines with various number of benzene rings. influence of the ionic conductivity, J. Mol. Liq. 328 (2021) 115471–115477, https://doi.org/10.1016/j.molliq.2021.115477.
[31] A.M. AbdelAty, D.A. Yousri, L.A. Said, A.G. Radwan, Identifying the parameters of Cole impedance model using magnitude only and complex impedance measurements: a metaheuristic optimization approach, Arabian J. Sci. Eng. 45 (8) (2020) 6541–6558, https://doi.org/10.1007/S13369-020-04532-4.
[32] K.S. Cole, R.H. Cole, Dispersion and absorption in dielectrics I. Alternating current characteristics, J. Chem. Phys. 9 (4) (1941) 341, https://doi.org/10.1063/1.1750906.